Progress In Electromagnetics Research, PIER 77, 193–214, 2007

DOUBLE STATISTICAL DISTRIBUTION OF CONDUCTIVITY AND ASPECT RATIO OF INCLUSIONS IN DIELECTRIC MIXTURES AT MICROWAVE FREQUENCIES

M. Y. Koledintseva, R. E. DuBroff, R. W. Schwartz and J. L. Drewniak

University of Missouri-Rolla
Rolla, Missouri, USA

Abstract—An analytical model of a composite dielectric presented in this paper is the extension of Maxwell Garnett formulation. It takes into account the simultaneous statistical (Gaussian) distribution of conductivity and aspect ratio of inclusions. The inclusions are randomly oriented elongated conducting spheroids at concentrations below the percolation threshold. The formulation presented herein is limited to microwave frequencies. However, taking subtle frequency-dependent effects that play important part at optical frequencies into account is straightforward. Some results of computations of microwave complex effective permittivity of composites with different input parameters have been obtained using analytical and numerical integration in Maple 10 software. It is shown how the parameters of the distribution laws — mean values and standard deviations of aspect ratio and conductivity — affect the resultant complex effective permittivity. The results of computations demonstrate that the most important factors affecting frequency characteristics of microwave effective permittivity are the mean values of the aspect ratio and conductivity. As for the standard deviations of aspect ratio and conductivity, their effects are the most noticeable in the transition between the static and optical limits of the Debye characteristic for the effective permittivity. There is almost no effect in the static and "optic" regions of the Debye curves.

Notations

$a = l/d$ - aspect ratio of the inclusions (ratio of the length to the diameter);

a_0 - mean value of the aspect ratio;

σ_a - standard deviation of the aspect ratio;

σ_e [S/m] - bulk conductivity of an inclusion;

σ_{e0} [S/m] - mean value of the bulk conductivity;

σ_c [S/m] - standard deviation for the bulk conductivity;

n [m^{-3}] - total concentration of inclusions;

f_i - volume fraction of the inclusions of the particular size and conductivity;

$N_{i1,2,3}$ - depolarization form factors of inclusions;

ε_b - relative permittivity of the base material;

ε_{eff} - effective permittivity of the composite material.

1. INTRODUCTION

This paper is a continuation of the study of frequency characteristics of composite dielectrics comprised of a dielectric base (host) material and conducting inclusions in the form of elongated spheroids [1, 2]. In paper [1], the model of the effective permittivity of composites containing conducting inclusions at optical frequencies was developed. This model is based on the Maxwell Garnett (MG) formulation and takes into account a number of subtle effects in metal inclusions in the optical range. These include the skin effect, the Drude frequency dependence, the effects related to the mean free path of electrons in nanometer-size conductors, as well as dimensional resonances and radiation associated with the length of inclusions. Some results of modeling in the optical range with statistically distributed aspect ratios of inclusions are also presented in [2]. It is shown that the wider standard deviation for aspect ratios broadens the bandwidth of absorption. It has also been shown that the shape and magnitude of an absorption curve depends on the mean value of the aspect ratio, the conductivity of inclusions, the concentration of inclusions, as well as the frequency characteristics of the base material.

It is known that in the composites with inclusions of lower conductivities, the maximum peak of absorption is observed at the lower frequencies. In contrast, the increase of conductivity

leads to the absorption peak shift to the higher frequencies [1–3]. To widen the bandwidth of absorptive properties of composites at both microwave and optical frequencies, it may be favorable to have mixtures of inclusions with different conductivities, including statistically distributed conductivities. From this point of view, it is important to consider the case, when both the aspect ratio and conductivity of inclusions are statistically distributed.

Engineering of microwave composite materials for different applications, such as electromagnetic shields, gaskets, printed circuit boards, microwave filtering devices, antenna radomes, etc., is an important practical problem [3–5]. The typical main requirements to shielding materials are their high shielding effectiveness, broadband performance, and omnidirectional behavior with respect to the angles of incidence of electromagnetic waves. Carbon inclusions are used as fillers in absorbing materials for microwave applications [3, 6–9], though properties of such materials have not been investigated extensively in the open literature. A peculiarity of carbon-filled composites is that the conductivity of carbon inclusions typically varies over a wide range, even if all carbon particles are obtained during the same technological process (e.g., exposed to burning during the same time). Hence, it is very important to know how the parameters of distribution laws — mean values and standard deviations of aspect ratio and conductivity — affect the resultant complex effective permittivity.

It should be mentioned that the optical frequency effect of statistical distribution of inclusion conductivity is also very important. Though most of the metals typically used as fillers of composites (Ag, Au, Pt, Al, Cu, etc.) at optical frequencies have more or less homogeneous bulk conductivity of inclusions [2], impurity and roughness of metal surfaces of inclusions lead to the increased statistical distribution of inclusion conductivities.

The objective of this paper is to include the abovementioned double statistical distribution in the Maxwell Garnett model, and thereby obtain computational results to study the main trends in frequency characteristics resulting from this double statistical distribution. Assume that all the inclusions are randomly oriented in the three-dimensional space, their concentration is below the percolation threshold, the size of inclusions is small compared to the wavelength, and, finally, the inclusions may neither move, nor change their shape and other parameters with time. These limitations allow for using the Maxwell Garnett formulation [10–12]. Herein, only microwave properties of composites are studied, where the Drude effect, the mean-free-path effect, and dimensional resonances [1] in the particles can be neglected. This facilitates retrieving the

basic effects associated with the double statistical distribution of the abovementioned parameters. However, skin effect in the inclusions may start playing an important part as frequencies increase (e.g., in the THz region), so in general it is taken into account. Also, for the sake of simplicity, the base dielectric is assumed here as lossless and non-dispersive.

Section 2 describes a mathematical model of the composite taking the double statistical distribution into account. The results of calculations based on this model are presented and discussed in Section 3. The conclusions are summarized in Section 4.

2. MATHEMATICAL MODEL

The Gaussian distribution law with respect to the bulk d.c. electric conductivity σ_e of conductive inclusions is

$$p(\sigma_e) = \frac{1}{\sqrt{2\pi}\sigma_c} \exp\left(-\frac{(\sigma_e - \sigma_{e0})^2}{2\sigma_c^2}\right), \tag{1}$$

where σ_{e0} is the mean bulk conductivity, and σ_c is the standard deviation for the conductivity.

If there is a double Gaussian distribution with respect to the conductivity σ_e and aspect ratio a, the two-dimensional probability density is

$$p(a, \sigma_e) = \frac{1}{2\pi\sigma_c\sigma_a} \exp\left(-\frac{(\sigma_e - \sigma_{e0})^2}{2\sigma_c^2}\right) \exp\left(-\frac{(a - a_0)^2}{2\sigma_a^2}\right), \tag{2}$$

where a_0 is the mean aspect ratio of inclusions, and σ_a is the standard deviation for aspect ratio.

The volume fraction of the inclusions for a particular conductivity σ_e and aspect ratio a is then proportional to the following two-dimensional probability density,

$$f_i(a, \sigma_e) = n v_i(a) p(a, \sigma_e), \tag{3}$$

where n is the concentration, consisting of the total number of inclusions per-unit-volume, and $v_i(a)$ is the volume of an individual inclusion.

Based on the MG representation given in [2], the effective

permittivity can be written as

$$\varepsilon_{ef} = \varepsilon_b + \frac{\frac{1}{3}\int\limits_{a_{\min}}^{a_{\max}}\int\limits_{\sigma_{e\min}}^{\sigma_{e\max}} \eta_i(\sigma_e)\varepsilon_b f_i(a,\sigma_e)\sum\limits_{k=1}^{3}\frac{1}{1+\eta_i(\sigma_e)N_{ik}(a)}d\sigma_e da}{1-\frac{1}{3}\int\limits_{a_{\min}}^{a_{\max}}\int\limits_{\sigma_{e\min}}^{\sigma_{e\max}} \eta_i(\sigma_e)f_i(a,\sigma_e)\sum\limits_{k=1}^{3}\frac{N_{ik}(a)}{1+\eta_i(\sigma_e)N_{ik}(a)}d\sigma_e da}, \tag{4}$$

where the coefficient

$$\eta_i(\sigma_e) = \frac{\varepsilon_i(\sigma_e)}{\varepsilon_b} - 1 \tag{5}$$

depends on the relative permittivities of the base material ε_b and the material of a conducting inclusion

$$\varepsilon_i(j\omega) = \varepsilon_i' - j\frac{\sigma_e}{\omega\varepsilon_0} \approx -j\frac{\sigma_e}{\omega\varepsilon_0}. \tag{6}$$

The limits of integration in (4) are chosen in a reasonable way for the Gaussian distribution as

$$\begin{aligned} a_{\min} &= a_0 - 3\sigma_a \quad \text{and} \quad a_{\max} = a_0 + 3\sigma_a; \\ \sigma_{e\min} &= \sigma_{e0} - 3\sigma_c \quad \text{and} \quad \sigma_{e\max} = \sigma_{e0} + 3\sigma_c. \end{aligned} \tag{7}$$

If the inclusions are in the form of elongated prolate spheroids (rods), their form factors in (4) can be calculated through their aspect ratio using the simplified formula derived based on formulations in [11, 13],

$$N_{i1} = N_{i2} = \frac{1-N_{i3}}{2};\ N_{i3} = \frac{1}{2}\cdot\frac{\ln\left(\frac{a+\sqrt{a^2-1}}{a-\sqrt{a^2-1}}\right)a - 2\sqrt{a^2-1}}{\left(\sqrt{a^2-1}\right)^3}. \tag{8}$$

When considering frequencies where the skin-effect is important, e.g., the THz frequency band, the mean bulk conductivity σ_{e0} in the above formulation should be replaced by the effective conductivity that takes the skin-effect into account, as in [14].

$$\begin{aligned} \sigma_{e0} \to \sigma_{skin} &= \sigma_{e0}\cdot\frac{1-j}{\Delta}\frac{J_1((1+j)\Delta)}{J_0((1+j)\Delta)}; \\ \Delta &= \frac{d}{2\delta_{skin}} = \frac{d}{2}\sqrt{\frac{\omega\mu_a\sigma_{e0}}{2}}; \end{aligned} \tag{9}$$

where J_0 and J_1 are the zero and first order Bessel functions of the first kind, and $\mu_a = \mu_0\mu_r$ is the absolute permeability of inclusions (if they are non-magnetic, then $\mu_a = \mu_0 = 4\pi\cdot 10^{-7}$ H/m).

3. RESULTS OF COMPUTATIONS

Some computational results for the effective permittivity of composite dielectrics at microwave frequencies with statistically distributed aspect ratios and conductivity of inclusions are presented in this Section. A diphasic mixture is considered. It is comprised of a base material, which is a non-dispersive dielectric (e.g., Teflon, $\varepsilon_b = 2.2$), and of conducting inclusions in the form of elongated spheroids (rods) corresponding to the depolarization form factors (8). The rods are assumed to be made of carbon. In these computations the skin-effect, dimensional resonances, and other subtle effects for conductivity in conducting inclusions are negligibly small.

Figure 1 demonstrates frequency dependence of the complex effective permittivity for two cases: (1) very narrow statistical distributions for both aspect ratio and conductivity (standard deviations are $\sigma_a = 1$ and $\sigma_c = 10\,\mathrm{S/m}$, respectively), and (2) both the aspect ratio and the conductivity of inclusions are statistically undistributed. It is seen from the figure that the corresponding real and imaginary parts of the effective permittivity practically coincide for

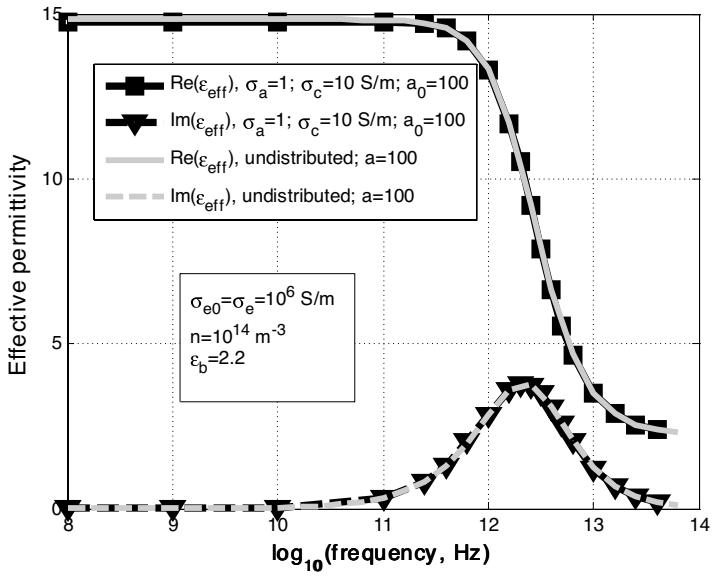

Figure 1. Frequency dependence of the effective permittivity for very narrow statistical distributions of both aspect ratio and conductivity, compared with the effective permittivity for an undistributed case (aspect ratio = 100, bulk conductivity of inclusion is $10^6\,\mathrm{S/m}$).

both cases. This expected result serves as a test for the computational correctness. The mean aspect ratio in the statistically distributed case is the same as the aspect ratio in the undistributed case ($a_0 = a = 100$), and the mean conductivity in the statistically distributed case is the same as in undistributed case $\sigma_{e0} = \sigma_e = 0$. The curves in Figure 1 obviously must be very close, since very narrow distributions converge to the undistributed case.

As is seen from Figure 1, the calculated frequency dependence for the real and imaginary parts of the effective permittivity follow the Debye law for dielectrics [15],

$$\varepsilon_{eff} = \varepsilon_{eff\infty} + \frac{\varepsilon_{eff\,s} - \varepsilon_{eff\infty}}{1 + j\omega\tau_{eff}}, \tag{10}$$

where $\varepsilon_{eff\,s}$ and $\varepsilon_{eff\infty}$ are the static and "optic" limit permittivities, τ_{eff} is the Debye relaxation constant, and $\omega = 2\pi \cdot f$ is the angular frequency. The parameters of the Debye (or Debye-like) curves — $\varepsilon_{eff\,s}$, $\varepsilon_{eff\infty}$, and τ_{eff} — can be simply estimated by visual inspection of the curves, or in slightly distorted cases may be easily extracted using optimization procedures based on the genetic algorithm, as described in [5, 16–18]. The Debye-like behavior of composites containing

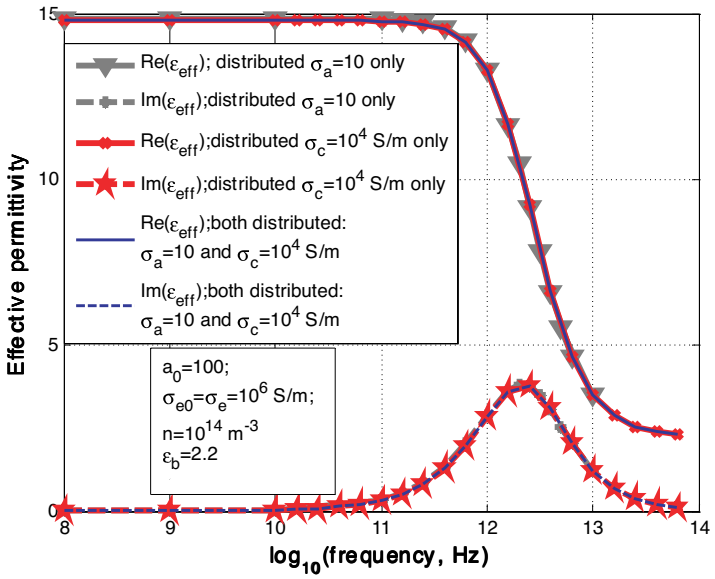

Figure 2. Comparison of effective permittivity curves for double statistical distribution and one of the distributions (aspect ratio only — narrow distribution, and conductivity only).

conducting rods may be explained by an analogy between the molecules of natural polar dielectrics and polarization of the induced dipoles in the inclusions of artificial dielectrics. Polarizability of an individual rod increases with the increase of its aspect ratio, and also with the increase of its bulk conductivity.

Figure 2 shows the frequency dependence of the effective permittivity for three different cases: (1) aspect ratio is distributed statistically with a comparatively low standard deviation ($\sigma_a = 10$), while conductivity is homogeneous ($\sigma_e = 10^6\,\mathrm{S/m}$); (2) the conductivity is statistically distributed ($\sigma_c = 10^4\,\mathrm{S/m}$), but the aspect ratio is homogeneous ($a = 100$); (3) both the aspect ratio and the conductivity of inclusions are distributed statistically ($\sigma_a = 10$ and $\sigma_c = 10^4\,\mathrm{S/m}$). The corresponding curves for all three cases almost coincide, because the statistical distribution of the aspect ratio is the dominant effect, and the corresponding standard deviation is comparatively narrow, close to the undistributed case. Also, it is seen that the standard deviation for conductivity might not affect the resultant effective permittivity characteristics. This hypothesis is tested below.

Figure 3 shows that the standard deviation of the aspect ratio has some impact on the effective permittivity of the composite. As

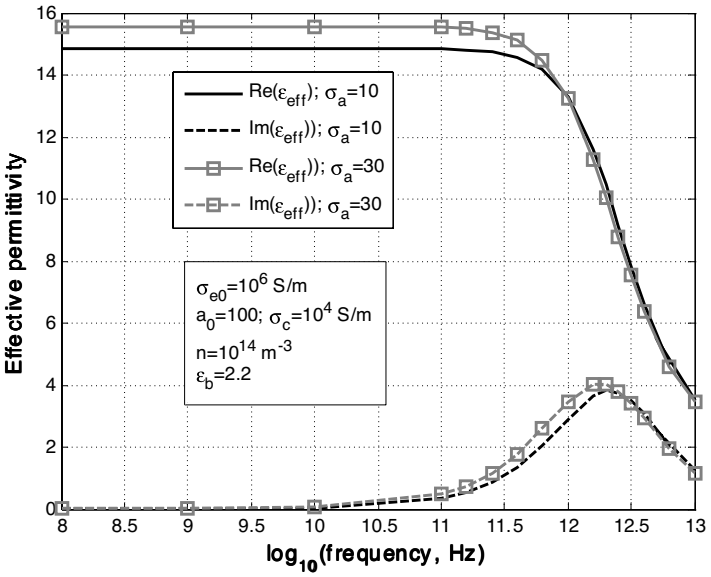

Figure 3. Effective permittivity curves for different standard deviations of the aspect ratio in the double Gaussian distribution.

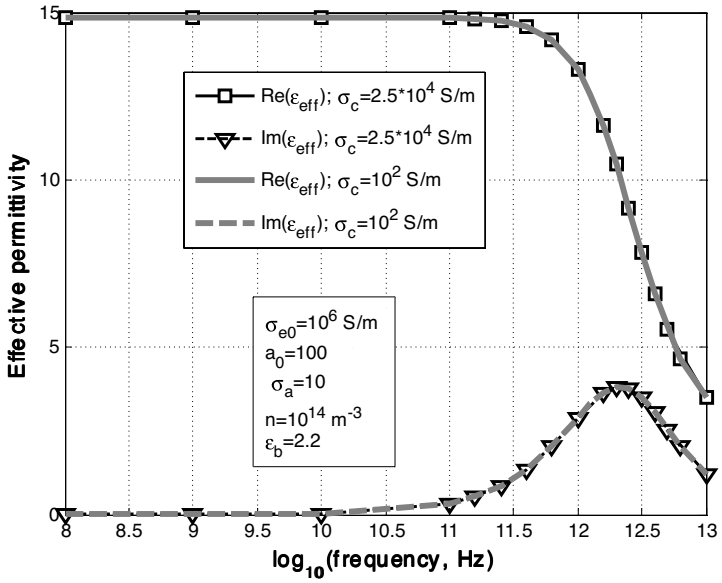

Figure 4. Effective permittivity versus frequency for different standard deviation of inclusion conductivity ($\sigma_c = 2.5 \cdot 10^4\,\mathrm{S/m}$ and $\sigma_c = 10^2\,\mathrm{S/m}$).

is seen from the figure, with the increase of the standard deviation σ_a, the magnitudes of the static relative effective permittivity and of the maximum loss increase slightly. It is also seen that the frequency dependence of the imaginary part becomes wider, and the frequency of the maximum loss shifts to the lower frequencies. This can be explained by the fact that σ_a determines the Q-factor of the material. When σ_a increases, the Q-factor decreases, and the corresponding frequency of the maximum loss shifts to the left.

Figure 4 shows that when the standard deviation is much smaller than the mean conductivity of inclusions $\sigma_c/\sigma_{e0} \ll 1$, the standard deviation of conductivity has almost no impact upon the effective permittivity characteristics. In Figure 4, there is almost no difference between the curves corresponding to $\sigma_c/\sigma_{e0} = 2.5 \cdot 10^{-2}$ and $\sigma_c/\sigma_{e0} = 10^{-4}$.

Figure 5 shows a pronounced effect of the mean value of the aspect ratio on frequency characteristics of the effective permittivity. The higher aspect ratios increase the values of the real static effective permittivity and the maximum loss. In addition, increasing the mean aspect ratio shifts the frequency of the maximum loss to the lower frequencies. This is an expected result. The mechanical

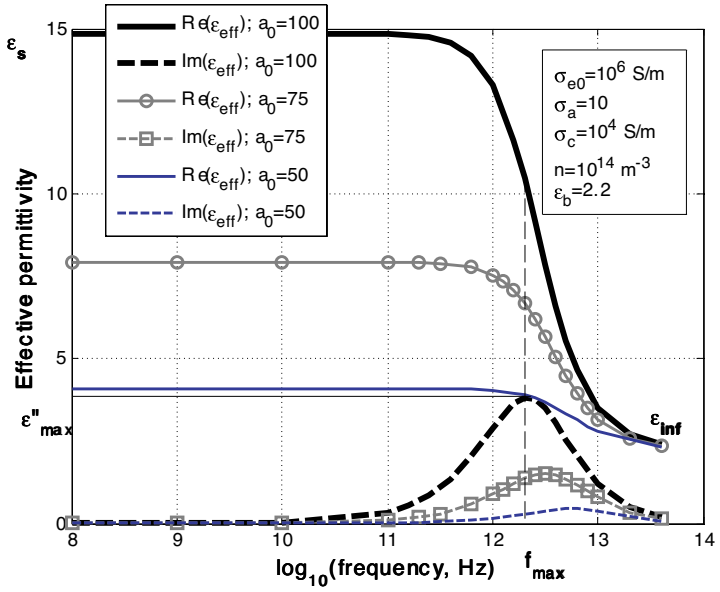

Figure 5. Frequency characteristics of effective permittivity for various values of the mean aspect ratio.

analogy with oscillating particles in a viscous liquid, which leads to the Debye frequency dependence, can explain this phenomenon. The dipole moment associated with an inclusion's polarizability is responsible for "inertia" at higher frequencies. The longer inclusions have more inertia, causing the decrease of the real part of the effective permittivity to occur at lower frequencies. The steepest slope of the real permittivity versus frequency corresponds to the frequency where the maximum in the curve for the imaginary part of permittivity takes place. This is the frequency of the maximum loss.

Figure 6 shows the effect of changing the concentration of inclusions. When the concentration of inclusions in the composite with the parameters indicated in Figure 6 increases by one order of magnitude (e.g., from 10^{14} to $10^{15}\,\mathrm{m}^{-3}$), the real static permittivity increases approximately five times. The maximum loss increases by a similar factor. However, a change in the concentration does not affect the frequency of the maximum loss. In all these cases the concentration used was below the percolation threshold.

Figure 7 demonstrates that there is a pronounced effect of the mean bulk conductivity of inclusions upon the effective permittivity curves. Though the static and "optic" values of real permittivity are

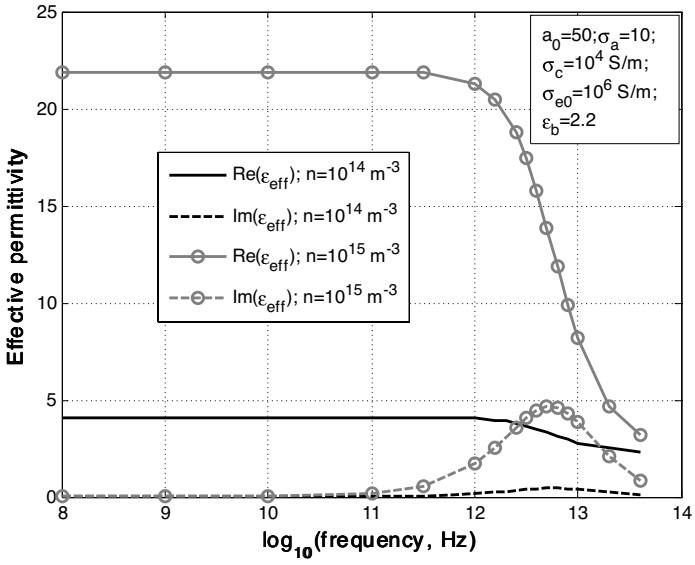

Figure 6. Frequency characteristics of effective permittivity for different inclusion concentrations.

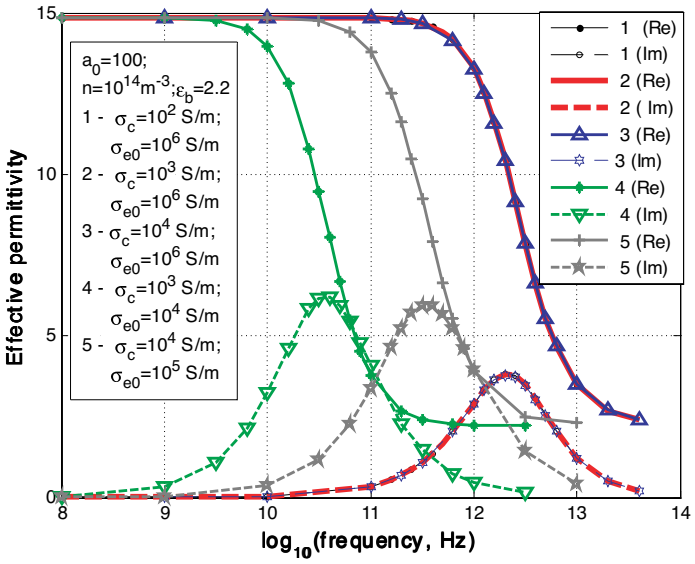

Figure 7. Effective permittivity frequency characteristics for different ratios of standard deviation to bulk conductivity of inclusions: 1- $\sigma_c/\sigma_{e0} = 10^{-4}$; 2- $\sigma_c/\sigma_{e0} = 10^{-3}$; 3- $\sigma_c/\sigma_{e0} = 10^{-2}$; 4- $\sigma_c/\sigma_{e0} = 10^{-1}$; and 5- $\sigma_c/\sigma_{e0} = 10^{-1}$.

nearly unaffected by the change in bulk conductivity, the frequency of the maximum loss for smaller conductivities is shifted to the lower frequencies, and the maximum loss (or ε''_{eff}) increases with the decrease of the bulk conductivity. This is also an expected result: the lower the conductivity, the lower is the frequency where the efficient absorption is observed [1, 3].

As is seen from Figure 7, the effect of the ratio of the standard deviation of conductivity to the mean bulk conductivity of inclusions (σ_c/σ_{e0}) is pronounced. The frequency of maximum loss is shifted to the lower frequencies for smaller conductivity. There is an effect of the ratio of the standard deviation to the bulk conductivity on the "tails" of the real effective permittivity frequency characteristics. For the first, second, and third curves, the ratio is $\sigma_c/\sigma_{e0} = 10^{-4}, 10^{-3}$, and 10^{-2}, respectively, while $\sigma_{e0} = 10^6$ S/m remains the same. These three curves almost do not differ, since the ratio σ_c/σ_{e0} remains small. The frequency of the maximum of loss is determined by $\sigma_{e0} = 10^6$ S/m, and it is $f = 10^{12.3} = 2 \cdot 10^{12}$ Hz. For the fourth curves, the bulk conductivity is minimal, $\sigma_{e0} = 10^4$ S/m, and the frequency of maximum loss is $f = 31.6$ GHz. For the ratio $\sigma_c/\sigma_{e0} = 10^{-1}$, the "tail" of the real part of the effective permittivity is elevated. The fifth curves are intermediate between the curves 1-3 and the curve 4, because the bulk conductivity in this case is $\sigma_{e0} = 10^5$ S/m. Since

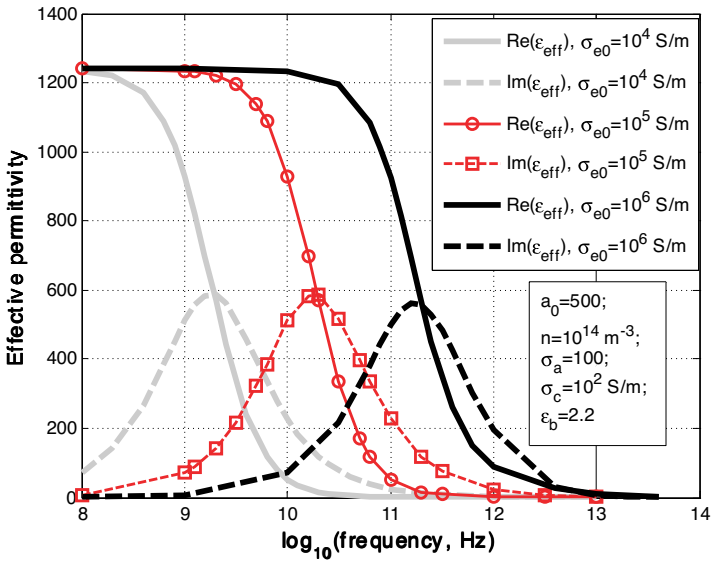

Figure 8. Effective permittivity as a function of frequency for different mean values of the inclusion conductivity.

the ratio $\sigma_c = \sigma_{e0} = 10^{-1}$ is the same as for the fourth curves, the distortion of the "tail" of the real part is also the same.

The effect of the mean bulk conductivity of inclusions on the effective permittivity curves is seen in Figure 8. The mean aspect ratio for the inclusions in this case is higher than in the previous graphs, $a_0 = 500$. The static real permittivity and the peak imaginary permittivity for $a_0 = 500$ are much higher ($\sim$75 times) than in Figure 7, where $a_0 = 100$. Three values of the bulk conductivity are considered: $\sigma_{e0} = 10^4, 10^5$, and 10^6 S/m. The standard deviation for conductivity is the same for all three sets of curves, and the deviation of the aspect ratio is also the same. As in the previous cases, the frequency of the maximum loss is shifted to lower frequencies for smaller values of the bulk conductivity. The maximum value of the imaginary permittivity ε''_{eff} increases slightly with the decrease of the bulk conductivity.

Figure 9 contains graphs of the effective permittivity as a function of the standard deviation of conductivity at three different frequencies: $f = 100$ MHz (static part of the Debye dependence, where $\varepsilon'_{eff} \approx \varepsilon_{eff\,s}$), $f = 2$ GHz (the slope of the Debye frequency characteristic, where $\varepsilon_{eff\,\infty} < \varepsilon'_{eff} < \varepsilon_{eff\,s}$, and $\varepsilon''_{eff} \approx \varepsilon''_{eff\,\max}$), and $f = 10^{12}$ Hz ("optic" limit in the Debye dependence, where $\varepsilon'_{eff} \approx \varepsilon_{eff\,\infty}$), respectively. As is seen from the figures, there is a significant effect of the standard deviation of conductivity only at the slope of the Debye curve, which corresponds to Figure 9 (b). This effect can be explained as follows. It is the mean bulk conductivity of an inclusion that is responsible for its polarizability. At the lower frequencies, all the inclusions-dipoles are agile enough to follow oscillations of the electric field. "Inertia" of the dipoles is not affected by the charges accumulated on the ends of the rods. At very high frequencies ("optic" limit) almost all dipoles, independently of conductivity, cannot follow very fast variations of the electric field, and they almost do not re-orient. This leads to the decrease of both ε'_{eff} and ε''_{eff}. However, when the frequency is at the slope of the Debye curve, where the dipoles partially follow the electric field, the effect of conductivity becomes more substantial. It is interesting that both real and imaginary parts of the effective permittivity decrease with the increase of the standard deviation of conductivity. This means that at the wider spread of conductivity, the higher fraction of inclusions become "heavier" compared to the case where conductivity of inclusions is homogeneous.

In Figures 10(a, b), showing the effective permittivity as a function of the mean aspect ratio, the graphs are calculated for three frequencies, corresponding to three regions of the Debye frequency dependence: $f = 10^8$ Hz (static permittivity), $f = 2 \cdot 10^{12}$ Hz (the steepest slope of the Debye dependence), and $f = 10^{13}$ Hz ("optic"

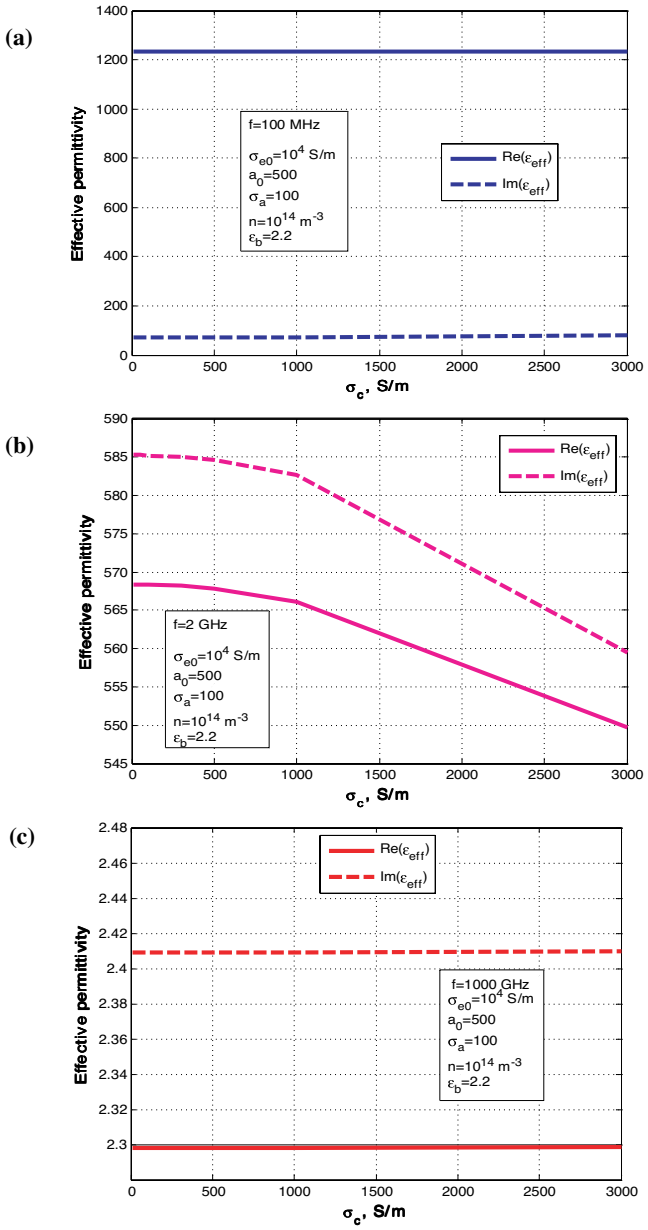

Figure 9. Effective permittivity as a function of the standard deviation of conductivity: (a) $f = 10^8$ Hz (static limit of the Debye dependence); (b) $f = 2 \cdot 10^9$ Hz (the steepest slope of the Debye dependence); (c) $f = 10^{13}$ Hz (the "optic" limit of the Debye dependence).

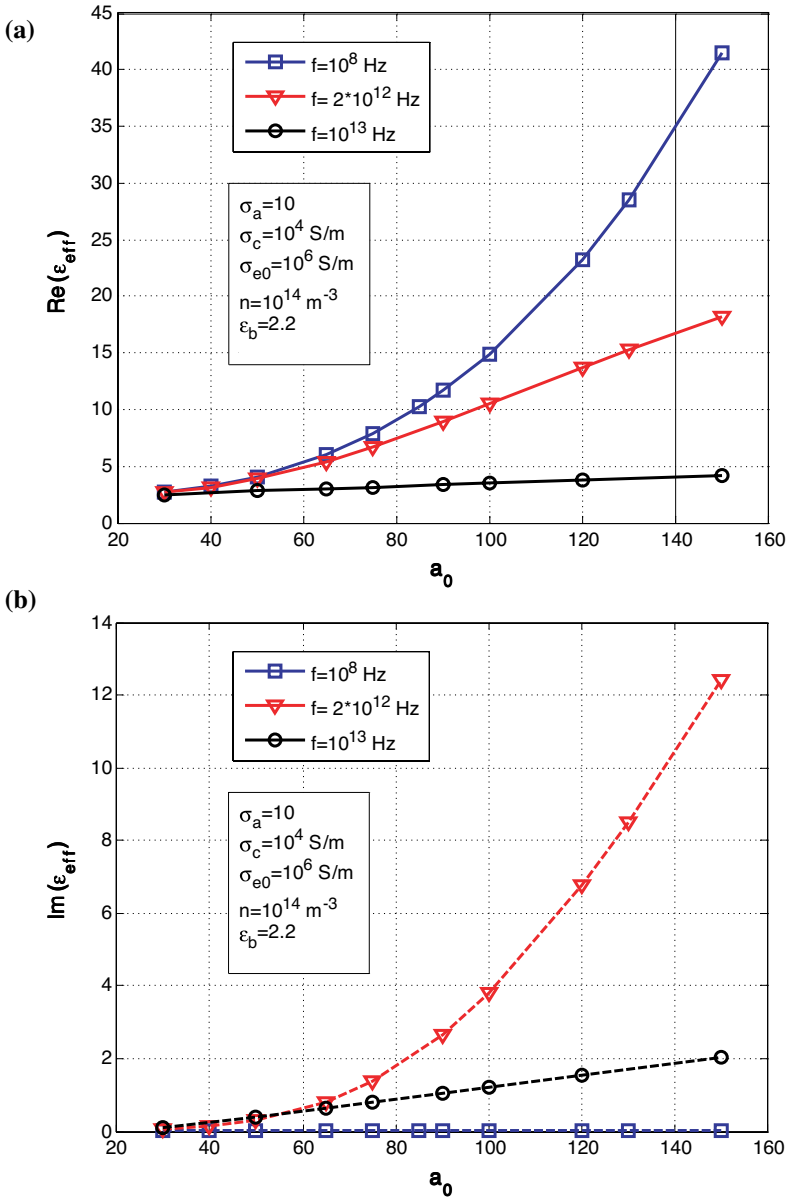

Figure 10. Dependence of the effective permittivity upon the mean aspect ratio: (a) real part of the effective permittivity; (b) imaginary part of the effective permittivity.

permittivity). The static permittivity $\varepsilon'_{eff} = \varepsilon_{eff\,s}$ dramatically increases when the mean aspect ratio becomes higher. This is a consequence of the increase of a dipole moment associated with the polarizability of a conducting rod as its aspect ratio increases (length increases and/or thickness decreases). The loss is relatively small in the static case $\varepsilon''_{eff\,s} \to 0$. In the "optic" limit, both the real ($\varepsilon'_{eff} = \varepsilon_{eff\,\infty}$) and imaginary ($\varepsilon''_{eff}$) permittivities increase slightly as the mean aspect ratio rises. As for the intermediate frequency range close to the slope of the Debye curve, the imaginary permittivity (ε''_{eff}) increases dramatically with the increase of the mean aspect ratio. The real permittivity ($\varepsilon'_{eff} = \varepsilon_{eff\,\infty}$) becomes higher, too. This phenomenon is related to the elevated polarizability effect, as well as the pronounced loss at the frequency where approximately half of the dipoles follow fast oscillations of electric field, and the other half have too much inertia to react. The absorption mechanism is associated with the imaginary part of the permittivity, and is related to the accumulation of electromagnetic energy within an inclusion and further dissipation of this energy into heat through multiple scattering. The real part of the permittivity is determined the polarization of dipoles. The dipoles that follow oscillations of the electric field, contribute to the real part of the effective permittivity and to the propagation effect in the dielectric. The dipoles that are "resistant" to oscillations, accumulate energy, which will eventually dissipate.

Figures 11 and 12 show how the standard deviation of the aspect ratio affects real and imaginary parts of the effective permittivity. Figures 11 and 12 differ by the values of the mean aspect ratio and bulk conductivity. In Figures 11, the values are $a_0 = 100$ and $\sigma_{e0} = 10^6$ S/m, and the frequency of the steepest slope (maximum loss) is around $2 \cdot 10^{12}$ Hz. In Figures 12, the values are $a_0 = 500$ and $\sigma_{e0} = 10^5$ S/m, and the frequency of the steepest slope (maximum loss) is around 16 GHz. The magnitudes of real and imaginary parts of the effective permittivity in Figures 12 are much higher than in Figures 11, because the mean aspect ratio in Figures 12 is five times greater. It is also seen from the graphs on both figures that the standard deviation of aspect ratio does not affect much the values of the effective permittivity. Static permittivity $\varepsilon'_{eff} = \varepsilon_{eff\,s}$ slightly increases with the increase of the standard deviation σ_a. "Optic" limit $\varepsilon'_{eff} = \varepsilon_{eff\,\infty}$ remains unchanged and comparatively low. Only when the frequency is at the steepest slope (maximum loss), the variation in the real permittivity becomes noticeable: ε'_{eff} slightly decreases in both cases.

Figures 13(a, b) show the linear dependence of the effective permittivity upon concentration of inclusions. In these computations,

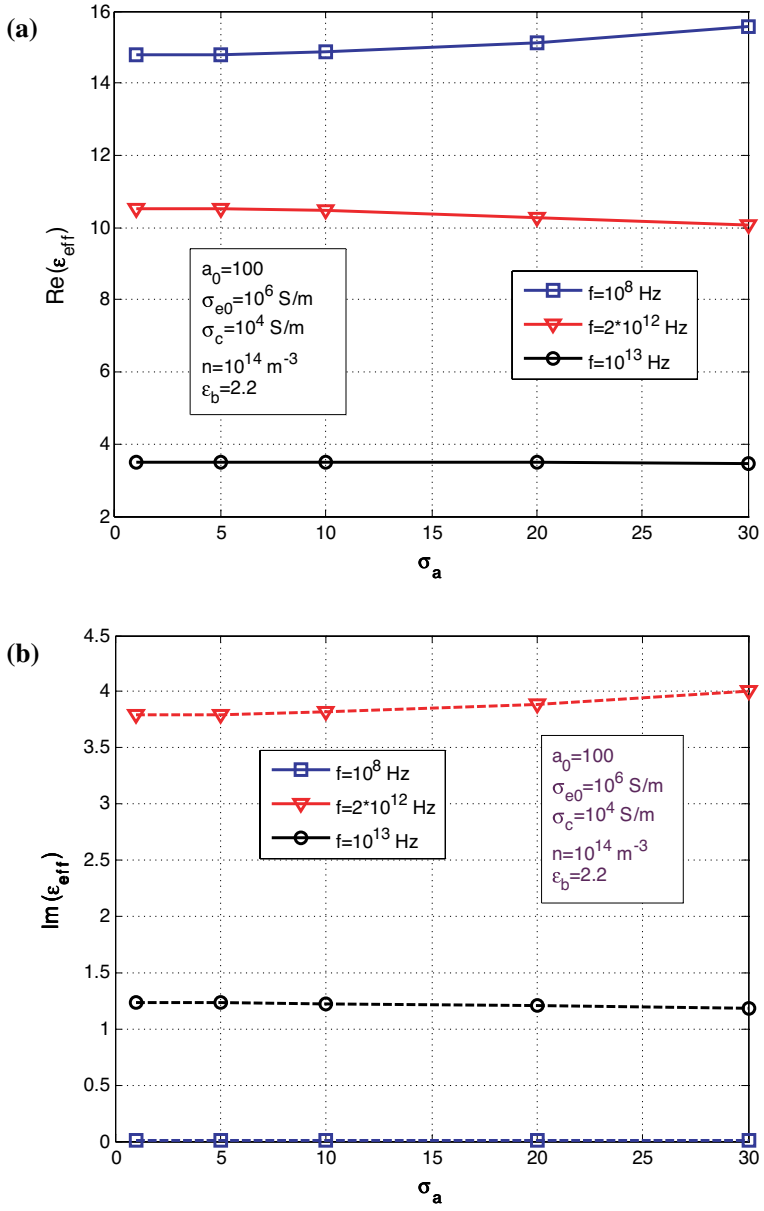

Figure 11. Dependence of the effective permittivity upon standard deviation of aspect ratio, when the mean aspect ratio is $a_0 = 100$, and the mean conductivity is $\sigma_{e0} = 10^6\,\mathrm{S/m}$: (a) the real part; (b) the imaginary part.

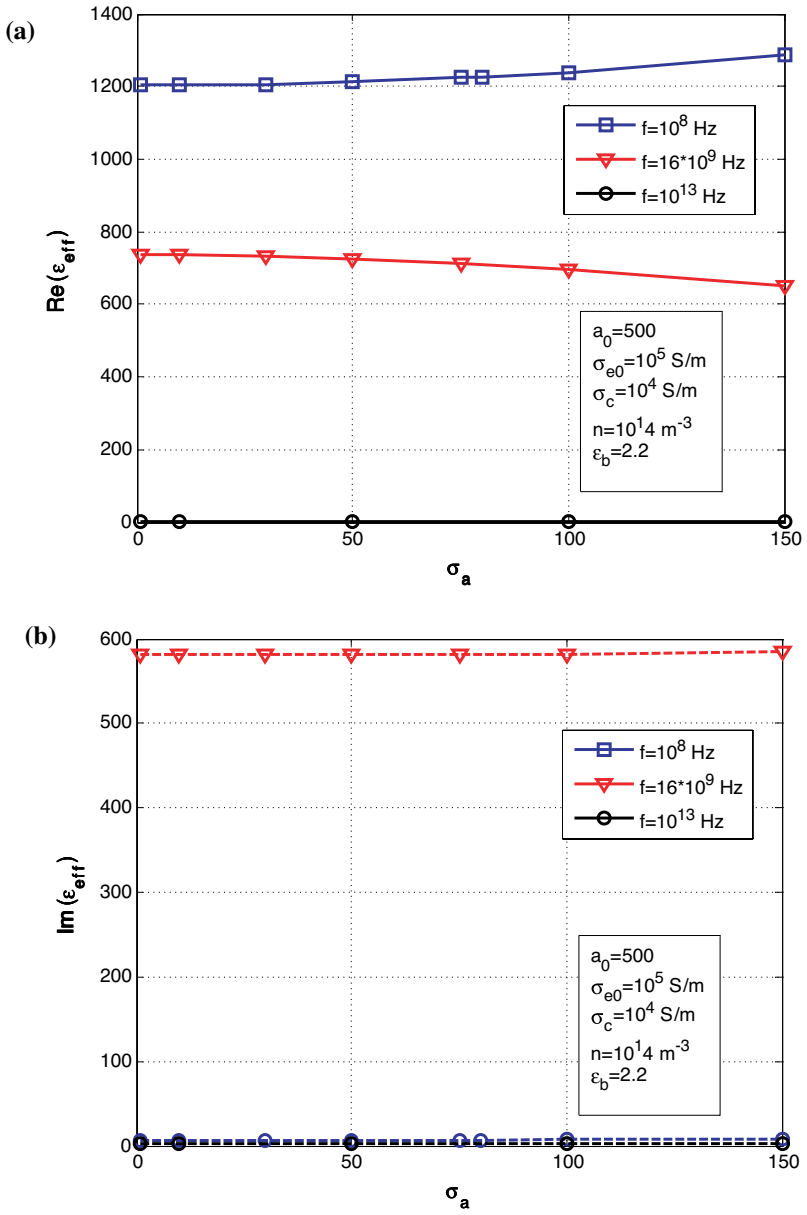

Figure 12. Dependence of the effective permittivity upon standard deviation of aspect ratio, when the mean aspect ratio is $a_0 = 500$, and the mean conductivity is $\sigma_{e0} = 10^5\,\mathrm{S/m}$: (a) the real part; (b) the imaginary part.

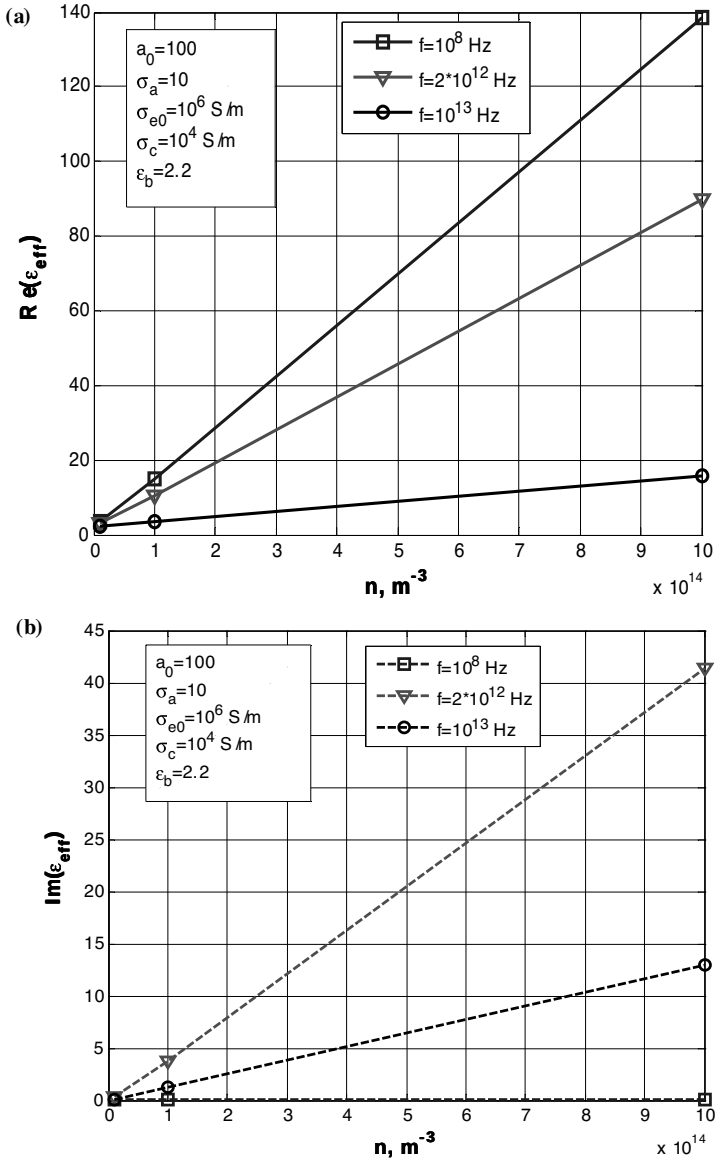

Figure 13. Dependence of the effective permittivity upon concentration of inclusions: (a) real part; (b) imaginary part. The graphs are calculated for three different frequencies: $f = 10^8$ Hz (static permittivity), $f = 2 \cdot 10^{12}$ Hz (steepest slope of the Debye dependence), and $f = 10^{13}$ Hz ("optic" permittivity).

the volume fraction of inclusions is still below the percolation threshold. For the composite with the mean aspect ratio of $a_0 = 100$ and the concentration of inclusions $n = 10^{14}\,\mathrm{m}^{-3}$, the calculated volume fraction of inclusions is around 0.4%, and for the concentration $n = 10^{15}\,\mathrm{m}^{-3}$, the volume fraction is around 4%. Assuming that the percolation threshold in this case is $p_c \approx 5/a = 5\%$, these concentrations of inclusions are still below the percolation threshold. The concentration affects most significantly the static real part of the effective permittivity $\varepsilon'_{eff} = \varepsilon_{eff\,s}$ and the imaginary part ε'_{eff} at the frequency of the maximum loss.

4. CONLUSIONS

In this paper, the Maxwell Garnett mixing rule is extended for a composite material containing conducting elongated spheroids (rods) with a double statistical distribution of aspect ratio and bulk conductivity of inclusions. This model includes normal (Gaussian) distribution functions instead of summations over the types of inclusions in the MG multiphase mixture formulation. The results of computations for microwave frequencies show that the mean values of the aspect ratio and the bulk conductivity of inclusions substantially affect frequency characteristics of composites. At the same time, standard deviations for the aspect ratio and conductivity only slightly change frequency characteristics, and these effects can be mostly observed closer to the frequency of the steepest slope (maximum loss) of the corresponding Debye curves for the effective permittivity of the composite.

ACKNOWLEDGMENT

This work was supported by the Air Force Research Laboratory under Contract FA8650-04-C-5704 through the Center for Advanced Materials Technology, University of Missouri-Rolla.

REFERENCES

1. Koledintseva, M. Y., R. E. DuBroff, and R. W. Schwartz, "A Maxwell Garnett model for dielectric mixtures containing conducting particles at optical frequencies," *Progress In Electromagnetics Research*, PIER 63, 223–242, 2006.
2. Koledintseva, M. Y., S. K. R. Chandra, R. E. DuBroff, and R. W. Schwartz, "Modeling of dielectric mixtures containing

conducting inclusions with statistically distributed aspect ratio," *Progress In Electromagnetics Research*, PIER 66, 213–228, 2006.

3. Koledintseva, M. Y., V. V. Bodrov, I. V. Sourkova, M. M. Sabirov, and V. I. Sourkov, "Unified spectral technique application for study of radiator behavior near planar layered composites," *Progress In Electromagnetics Research*, PIER 66, 317–357, 2006.
4. Amirhosseini, M. K., "Three types of walls for shielding enclosures," *Journal of Electromagnetic Waves and Apllications*, Vol. 19, No. 6, 827–838, 2005.
5. Park, H. S., I. S. Choi, J. K. Bang, S. H. Suk, S. S. Lee, and H. T. Kim, "Optimized design of radar absorbing materials for complex targets," *Journal of Electromagnetic Waves and Apllications*, Vol. 18, No. 8, 1105–1117, 2004.
6. Calame, J. P. and W. G. Lawson, "A modified method for producing carbon-loaded vacuum-compatible microwave absorbers from a porous ceramic," *IEEE Trans. Electron. Devices*, Vol. 38, No. 6, 1538–1543, June 1991.
7. Neo, C. P. and V. K. Varadan, "Optimization of carbon fiber composite for microwave absorber," *IEEE Trans. Electromagn. Compat.*, Vol. 46, No. 1, 102–106, Feb. 2004.
8. Ezquerra, T. A., F. Kremer, and G. Wegner, "AC electrical properties of insulator-conductor composites," *Progress In Electromagnetic Research*, PIER 06, 273–301, 1992.
9. Nedkov, I., S. Kolev, S. Stavrev, P. Dankov, and S. Alexsandrov, "Polymer microwave absorber with nanosized ferrite and carbon fillers," *Proc. IEEE 27th Int. Spring Seminar on Electronics Technology*, 577–579, 2004.
10. Maxwell Garnett, J. C., "Colours in metal glasses and metal films," *Philos. Trans. R. Soc. London, Sect. A*, Vol. 3, 385–420, 1904.
11. Sihvola, A., *Electromagnetic Mixing Formulas and Applications*, IEE, London, UK, 1999.
12. Xu, X., A. Qing, Y. B. Gan, and Y. P. Feng, "Effective properties of fiber composite materials," *Journal of Electromagnetic Waves and Apllications*, Vol. 18, No. 5, 649–662, 2004.
13. Landau, L. D., E. M. Lifshitz, and L. P. Pitaevskii, *Electrodynamics of Continuous Media*, 2nd edition, Pergamon, Oxford, New York, 1984.
14. Lagarkov, A. N. and A. K. Sarychev, "Electromagnetic properties of composites containing elongated conducting inclusions," *Phys. Review B*, Vol. 53, No. 9, 6318–6336, March 1996.

15. Von Hippel, A., *Dielectrics and Waves*, Artech House, Boston, London, 1995.
16. Koledintseva, M. Y., J. Wu, J. Zhang, J. L. Drewniak, and K. N. Rozanov, "Representation of permittivity for multi-phase dielectric mixtures in FDTD modeling," *Proc. IEEE Symp. Electromag. Compat.*, Vol. 1, 309–314, Santa Clara, CA, Aug. 9–13, 2004.
17. Meng, Z.-Q., "Automonous genetic algorithm for functional optimization," *Progress In Electromagnetic Research*, PIER 72, 253–268, 2007.
18. Donelli, M., S. Caorsi, F. de Natale, D. Franeeschini, and A. Massa, "A versatile enhanced genetic algorithm for planar array design," *Journal of Electromagnetic Waves and Apllications*, Vol. 18, No. 11, 1533–1548, 2004.